Pancreatology 16 (2016) 337–346

Contents lists available at ScienceDirect

Pancreatology

journal homepage: www.elsevier.com/locate/pan

Original article

Regulation of autophagy by systemic admission of microRNA-141 to target HMGB1 in L-arginine-induced acute pancreatitis in vivo

Hongwei Zhu [a], Lihua Huang [b], Shaihong Zhu [a], Xia Li [c], Zhiqiang Li [a], Can Yu [a], Xiao Yu [a, *]

[a] Department of Hepatopancreatobiliary Surgery, Third Xiangya Hospital, Central South University, Changsha 410013, China
[b] Center for Medical Experiments, Third Xiangya Hospital, Central South University, Changsha 410013, China
[c] Department of Endocrinology, Third Xiangya Hospital, Central South University, Changsha 410013, China

ARTICLE INFO

Article history:
Available online 15 March 2016

Keywords:
Acute pancreatitis
Autophagy
microRNA-141
Gene therapy

ABSTRACT

Background & aims: MicroRNAs are endogenous, non-coding RNAs of approximately 20–22 nucleotides that regulate gene expression by binding to the 3′ untranslated region (UTR) of target mRNAs and can be applied in gene therapy. Acute pancreatitis is an inflammatory pancreatic disease that carries considerable morbidity and mortality. The purpose of this study was to explore the therapeutic potential of microRNA-141 (miR-141) for acute pancreatitis in vivo.

Methods: AP was induced by two hourly intra-peritoneal (i.p.) injections of L-arginine (200mg × 2/100 g.BW). Control mice received normal saline injections. In a separate group, normal saline, empty adenoviral vector and miR-141 adenoviral vector were given to the mice via tail vein hydrodynamically at 72 h before the first L-arginine injection. All the mice were euthanized at 24 h after the last L-arginine injection, and the pancreatic tissues were assessed by qRT-PCR, Western blotting and electron microscopy.

Results: miR-141 directly inhibited HMGB1 expression in mouse hepal-6 cell. Furthermore, systemic administration of the miR-141 knock-down the expression of HMGB1 protein and further antagonized the downstream protein Beclin-1, leading to the reduction of autophagosomes and autolysosomes, blockade of the LC3-II level and the increased levels of p62 protein after injection of L-arginine. In addition, the level of Lamp-2 was not significantly different.

Conclusions: For the first time miR-141 was applied in acute pancreatitis treatment in vivo. Inhibition of HMGB1 by miR-141 may block the process of autophagosome formation through the HMGB1/Beclin-1 pathway. The miR-141 appears to be a promising candidate for the gene therapy of acute pancreatitis.

Introduction

MicroRNAs (miRNAs) are small, non-protein-coding, single-stranded RNAs that regulate target gene expression post-transcriptionally in normal tissues and cancers. MiRNA binds to the 3′ UTR of target gene mRNA, leading to the repression or degradation of the transcript through imperfect or perfect complementarity. The partial complementarity allows miRNA to target 3′ UTR of multiple gene [1–3], and growing evidences indicate that miRNAs are involved in a range of processes including cellular development, apoptosis and autophagy [4–7]. A recent study demonstrates that hydrodynamics-based gene delivery into mice by intravenous administration of naked plasmid DNA is a more efficient procedure for expressing cytokines in *vivo* [8], suggesting that systemic admission of microRNA-141 may be an effective tool for gene therapy [9].

Acute pancreatitis (AP) is a poorly understood inflammatory disease, responsible for significant human morbidity and mortality worldwide each year [10]. Novel therapeutic approaches are needed to improve the long-term survival for this disease. Recent advances in the understanding of the altered gene expression and signaling pathways in acute pancreatitis offer the opportunities for new therapeutic strategy targeting essential molecular mechanisms.

HMGB1 (high mobility group box 1) belongs to a family of highly conserved proteins that contain HMG box domains. HMGB1 is a ubiquitous nuclear protein that regulates and facilitates various

* Corresponding author. Department of hepatopancreatobiliary Surgery, Third Xiangya Hospital, Central South University, Changsha, Hunan 410013, China. Tel.: +86 1307 7304048; fax: +86 0731 88618612.
E-mail address: yuxiaoyx4@126.com (X. Yu).

http://dx.doi.org/10.1016/j.pan.2016.03.004
1424-3903/

DNA-related activities such as transcription, replication, recombination and repair. In addition to its functions in the nucleus, HMGB1 plays a significant extracellular role in inflammation and immunity [11,12]. In patients and animals with AP, the serum HMGB1 levels are significantly increased and positively correlate with the severity of the disease [13–15]. Inhibiting the release or cytokine activity of HMGB1 confers protection against experimental AP [16–18]. However, the precise role of HMGB1 during acute pancreatitis-induced tissue injury and subsequent local and systemic inflammation is poorly understood.

In this study, we examined the impact of miR-141 on HMGB1 expression and its molecular action in the regulation of autophagy in acute pancreatitis. Our study suggests that miR-141, repressing the expression of HMGB1, reduces autophagosomes and autolysosomes, decreases LC3-II level and increases levels of p62 protein after injection of L-arginine. These findings indicate that the miR-141, repressing the HMGB1 expression, attenuates L-arginine-induced acute pancreatitis.

Materials and methods

Plasmid construction

A 600-base-pair genomic fragment spanning the mmu-miR-141(GenePharma company, Shanghai, China) was inserted into pUC19 expression vector (Genscript Biotechnology Company, Nanjing, China) at its *Xho*I/*Bgl*II sites to express miR-141. The whole sequence was confirmed by DNA sequencing. The empty expression plasmid was designated as control. Plasmids were prepared using Endo-free Plasmid Giga kit (Qiagen, Germantown, MD, USA) according to the manufacturer's direction. The primer sequences of miR141 were as follows: forward-5′-CGCGGATCCACCCT-GAGCTCTGCCACCG-3′, reverse-5′- CGGAATTCGCAGCAGGATGG-CAGGCAGAC-3′.

Cell culture and transfection

Mouse hepatoma cell line hepal-6 was acquired from Institute of Biochemistry and Cell Biology, Chinese Academy of Sciences. Cells were cultured in Dulbecco's modified Eagle's medium (DMEM) supplemented with 10% FBS at 37 °C under 5% CO_2 in atmosphere. MiR-141 and control plasmids (2 μg each) were transfected into cells seeded in six-well plates by Fugene HD Transfection Reagent (RocheApplied Science, Indianapolis, IN, USA) following the manufacturer's instruction.

RNA isolation and qRT-PCR

Total RNA was extracted by using Trizol (Invitrogen) according to the manufacturer's instructions and reverse transcribed for quantification using the TaqMan microRNA Reverse Transcription Kit (Applied Biosystems) according to the manufacturer's instructions. Mature miRNAs were quantified using 2-step TaqMan qRT-PCR with the TaqMan microRNA kit. MiRNA expression level was normalized using U6 RNA as an internal control. qRT-PCR for HMGB1 with specific primers from SABiosciences was performed using a RT2 First Strand Kit (SABiosciences) according to the manufacturer's instructions. Fold changes of mRNA levels in target gene relative to the POLR2A (RNA polymerase II) control were calculated by relative quantification analysis. The PCR primers used were as follow: 5-TGCGGGTGCTCGCTTCGGCAGC-3′ (sense) and 5′-CCAGTG-CAGGGTCCGAGGT-3′ (antisense) for U6 and 5′-CCTCGCGTAA-CACTGTCTGGTAA-3′ (sense) and 5′-GTGCAGGGTCCGAGGT-3′ (antisense) for microRNA-141 and 5′-CCCCAAAATCAAAGGCGAGC-3′ (sense) and 5′- TCTGCTGCAGTGTTGTTCCA-3′ (antisense) for HMGB1 and 5′-AGGCGAAACCAGGAGAGACC-3′ (sense) and 5′-ACAC-CATCCTGGCGAGTTTC-3′ (antisense) for Beclin-1.

Luciferase reporter assay

HMGB1 3′UTR Lenti-reporter-Luciferase Vector was obtained from ABM. This HMGB1 3′UTR-containing vector (pLenti-UTR-Luc) was used as a template to create mutated miR-141 binding sites (HMGB1-UTRmt) by using the GeneArt® Site-Directed Mutagenesis PLUS System (Invitrogen, A14604) according to the manufacturer's instructions. Hepal-6 cells were seeded in 24-well plates 1 day before transfection. Antagomir and mimic of miR141, non-target antagomir and mimic of control, purchased from GenePharma company, were transiently transfected into the cells together with the luciferase reporter constructs described above (200 ng) and pRL-CMV(20 ng). After 48 h, the luciferase activity was determined using the dual luciferase reporter assay system (Promega). The relative reporter activity was obtained by normalization to the Renilla luciferase activity. All experiments were performed in triplicate.

Western blotting analysis

Cells transfected for 48 h were lysed on ice for 30 min by RIPA Lysis Buffer (Beyotime Biotechnology, China). For tissue samples, the frozen tissue was powdered in liquid nitrogen and lysed in RIPA lysis buffer. Equal-dose protein from each sample was applied to SDS–PAGE gel and probed with specific antibodies including HMGB1, Beclin-1, p62, Lamp-2, LC3 and β-actin as control (Sigma, St Louis, MO, USA).

Viral vector production

Recombinant adenoviral vectors expressing EGFP (pYr-adv-mmu-miR141) were generated following standard techniques. The pAd/PL-DEST™ adenoviral vector system (Yingrun Biotechnology Co Ltd, Changsha, China) was used. The adenoviral plasmids were produced by homologous recombination in competent DH5a cells between the adenoviral backbone plasmid vector, pAd/PL-DEST, and a shuttle vector pAdTrack. The pAdTrack vector is a shuttle vector for production of EGFP-trackable viral vectors. The adenoviral vectors were then produced by transfection in HEK293 cells. At last, the recombinant adenovirus titer reached 1×10^{11} PFU/ml.

Animal experiments

All animal protocols were approved by the Institutional Animal Care and Treatment Committee of Central south of University (Changsha, Hunan, China). The mice strain is Kunming (KM), a breeding in China with white color for easy tail injection. For induction of AP, Kunming mice were given two hourly intraperitoneal (i.p.) injections of L-arginine (200mg × 2/100 g.BW). The control mice received equal volume and frequency of normal saline injections. Five mice were assigned to each group. Animals were then sacrificed one day (24 h) after the last L-arginine injection, and the pancreas were harvested. In a separate experiment, normal saline (NS group), empty adenoviral vector (Ad-miR-ctrl group) and miR-141 adenoviral vector (Ad-miR-141 group) were given to the mice via tail vein hydrodynamically at 72 h before the first L-arginine injection. In addition, control mice received normal saline via tail vein hydrodynamically while not receiving L-arginine injection. Five mice per group were assigned to NS group, NS + L-arginine group, Ad-miR-ctrl + L-arginine group and Ad-miR141 + L-arginine group. The mice were euthanized 24 h after the last L-arginine injection, and pancreatic tissue samples were collected,

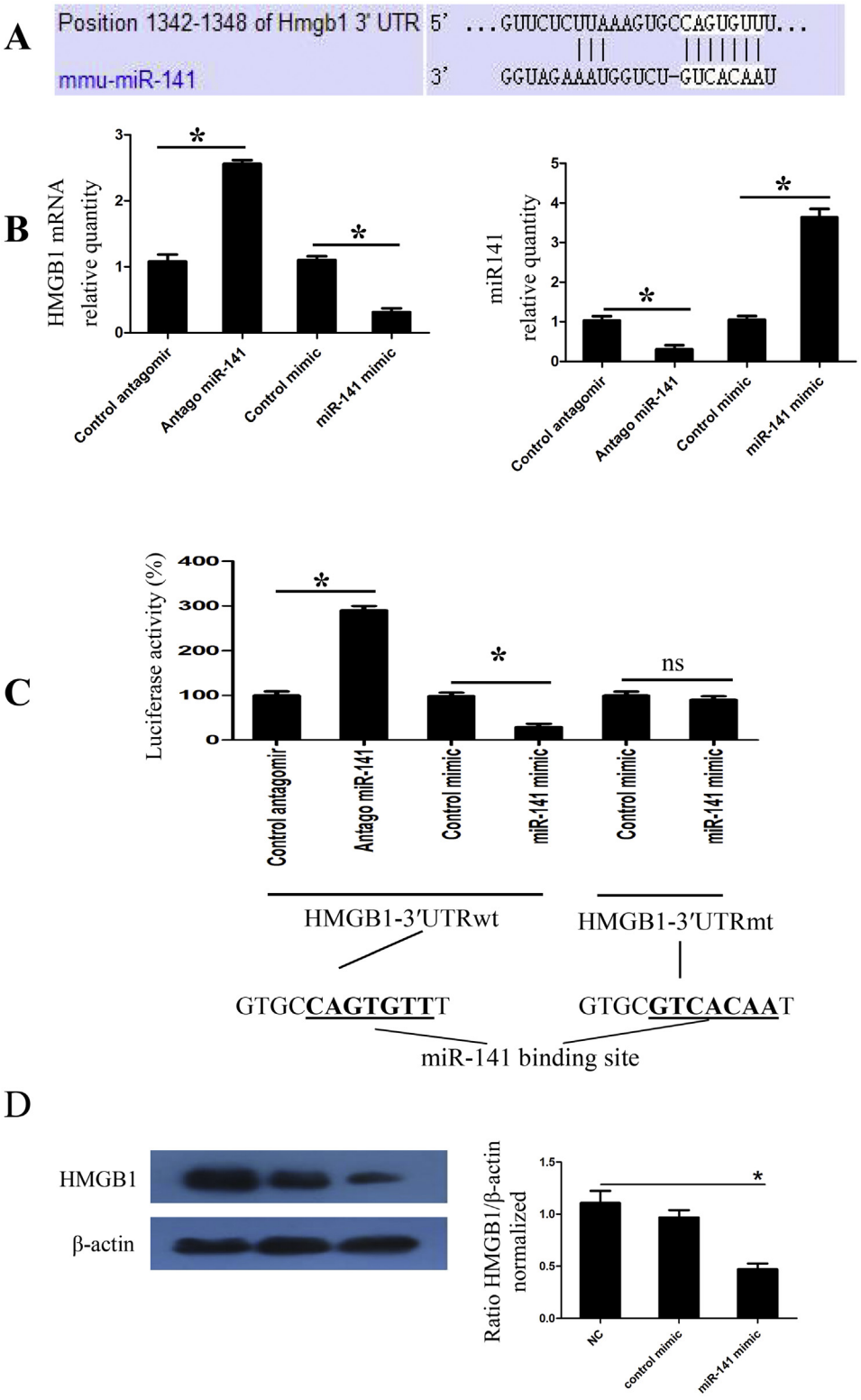

Fig. 1. MicroRNA-141 targets HMGB1. (**A**) Schema representing the functional interaction between miR-141 and the seed sequence (bold) in the 3′UTR of HMGB1 mRNA as predicted by online software for microRNA targets. (**B**) Mouse hepal-6 cells were transfected with antagomir or mimic of miR-141 or non-target antagomir or mimic control (100 nM) for 72 h, and the level of miR-141 was assayed by qRT-PCR. In parallel, the mRNA level of HMGB1 was assayed by qRT-PCR ($n = 5$, $^*P < 0.05$). Data represent relative level, with control set as 1. (**C**) Luciferase assay of Hepal-6 cells co-transfected with reporter constructs containing HMGB1 3′ UTRs with (HMGB1-UTRwt) or without (HMGB1-UTRmt) miR-141-binding sites and mimic of miR-141 or scrambled control for 72 h ($n = 5$, $^*P < 0.05$; ns, non-significant). Data represent relative level, with control set as 100%. (D) Mouse hepal-6 cells were transfected with mimic of miR-141 or mimic control (100 nM) for 72 h, and the protein expression of HMGB1 was determined by western blot analysis.

snap-frozen in liquid nitrogen, and stored at −80 °C for Western blotting. In addition, frozen pancreatic tissues were fixed in ice-cold 1.5% paraformaldehyde for electron microscopy observation.

Electron microscopy observation

Frozen pancreatic tissues ($n = 5$) were fixed in ice-cold 1.5% paraformaldehyde and embedded in Epon resin (Sigma–Aldrich, St. Louis, MO). Ultrathin sections were prepared for microscopy according to a routine procedure. Areas within scanned images of electron micrographs were measured using a Metamorph tracing semi-automatic counting tool. The autophagosomes and autolysosomes were carefully outlined and the area within the traced region was determined using the analySIS 3.2 Software (Soft Imaging System, Munster, Germany) and expressed in square nanometers. All areas in a section were added together and calculated as a percentage of the entire region measured, and were digitally evaluated in 5 animals per group ($n = 5$) in 100 randomly selected $45 \times 45\ \mu m^2$ fields per animal.

Statistical analysis

All data were analyzed using SPSS version 19.0 (SPSS, Chicago, IL, USA) and expressed as mean ± SD. Differences between groups were compared by one-way analysis of variance and *t*-test. A value of $P < 0.05$ was considered statistically significant.

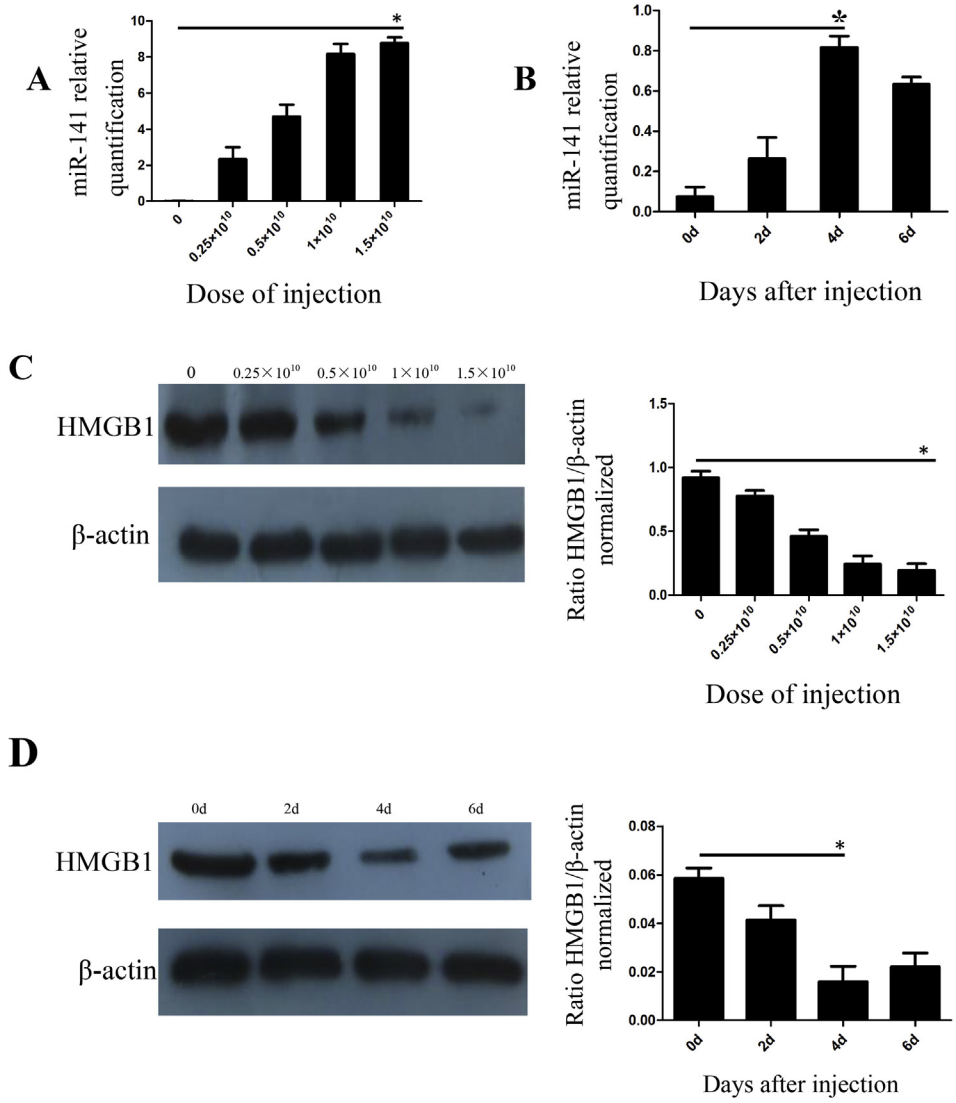

Fig. 2. MicroRNA-141 is transfected in mice pancreatic tissue and down-regulates the expression of HMGB1. **(A)** Various amounts of pYr-adv-mmu-miR141 from 1×10^{10} PFU to 1.5×10^{10} PFU were injected into mice ($n = 5$ for each dose) within 5 s. Pancreatic tissues were collected 96 h after injection. MicroRNA-141 levels were determined by qRT-PCR. The values represent the mean ± SD. $^*P < 0.05$, significantly different from the values at dose 0. **(B)** Temporal pattern of microRNA-141 expression after intravenous injection of microRNA-141. 1×10^{10} PFU pYr-adv-mmu-miR141 was injected into mice ($n = 5$) within 5 s. Pancreatic tissues were collected at 0, 2, 4, and 6 days after miR-141 injection. MicroRNA-141 levels were determined by qRT-PCR. The values represent the mean ± SD. $^*P < 0.05$, significantly different from the values at day 0 (before injection). **(C)** Various amounts of pYr-adv-mmu-miR141 from 1×10^{10} PFU to 1.5×10^{10} PFU were injected into mice ($n = 5$ for each dose) within 5 s. Pancreatic tissues were collected 96 h after injection. HMGB1 levels were determined by Western blotting. The values represent the mean ± SD. $^*P < 0.05$, significantly different from the values at dose 0. **(D)** Temporal pattern of HMGB1 expression after intravenous injection of microRNA-141. 1×10^{10} PFU pYr-adv-mmu-miR141 was injected into mice ($n = 5$) within 5 s. Pancreatic tissue was collected at 0, 2, 4, and 6 days after miR-141 injection. HMGB1 levels were determined by Western blotting. The values represent the mean ± SD. $^*P < 0.05$, significantly different from the values at day 0 (before injection).

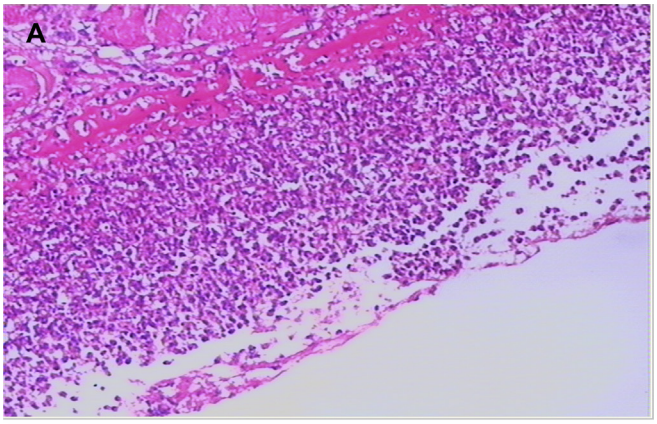

L-argine (HE, ×100)

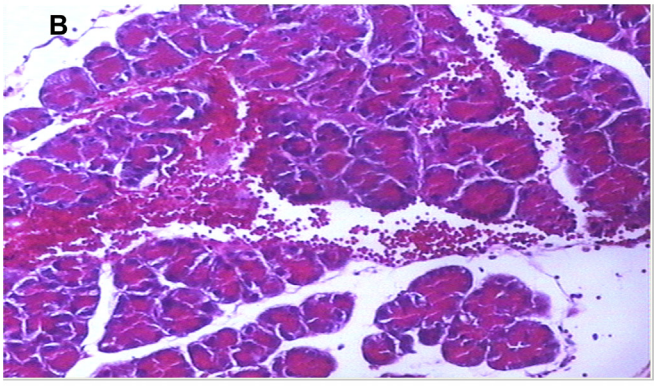

NS (HE, ×100)

Fig. 3. Histologic assessment of acute pancreatitis tissues in response to L-arginine**(A)**, normal saline (**B**), stained with H&E. Note the large areas of vacuoles within the acute pancreatitis tissue. Original magnification: 100×.

Results

HMGB1 is a target of miR-141 in mouse hepal-6 cell

Based on the miRNA database, HMGB1 is a predicted miR-141 target in mice. It was shown that the 3′UTR of HMGB1 contains a potential binding site for miR-141 (Fig. 1A). To determine the effect of miR-141 on the expression of HMGB1, we used miR-141 mimic and antagomiR-141 to modulate the cellular miR-141 levels (Fig. 1B). The mRNA level of HMGB1 decreased following miR-141 mimic treatment, whereas antagomiR-141 increased HMGB1 expression. The activity of HMGB1 3′ UTR was further assessed by luciferase reporter assays (Fig. 1C). MiR-141 mimic inhibited the luciferase activity with HMGB1-UTRwt in hepal-6 cell. In contrast, miR-141 mimic had no effect on the expression of luciferase reporter regulated by mutated miR-141 binding sites (HMGB1-UTRmt). Consistently, the protein levels of HMGB1 decreased following miR-141 mimic treatment in mouse hepal-6 cell (Fig. 1D). These findings suggest that HMGB1 is the target of miR-141 in mouse hepal-6 cell.

MicroRNA-141 is transfected into pancreatic tissues successfully and down-regulates the expression of HMGB1

To determine whether pYr-adv-mmu-miR141 is transfected in mice pancreatic tissues successfully, mice were injected with various amounts of pYr-adv-mmu-miR141 hydrodynamically, and their pancreatic tissues were collected 96 h later (Fig. 2A). The microRNA-141 levels in the pancreatic tissue clearly increased in an ad-miR141 dose-dependent manner. Increasing the amount of injected pYr-adv-mmu-miR141 from 1×10^{10} PFU to 1.5×10^{10} PFU per mouse did not further increase the pancreatic microRNA-141 level. To evaluate the temporal pattern of microRNA-141 expression after the hydrodynamics-based pYr-adv-mmu-miR141 delivery, samples were collected at various time points after the injection of pYr-adv-mmu-miR141 at 1×10^{10} PFU per mouse (Fig. 2B). The microRNA-141 level in pancreatic tissue of mice with pYr-adv-mmu-miR141 treatment was at the peak point 4 days after the injection.

Meanwhile, the pancreatic HMGB1 level was gradually decreased, reaching the maximum extent at day 4, and rebounded a little at day 6 due to possible miRNA degradation. To examine the dose dependency of HMGB1 expression following hydrodynamics-based pYr-adv-mmu-miR141 delivery, mice were injected with various amounts of pYr-adv-mmu-miR141 and their pancreatic tissues were collected 96 h later. Pancreatic tissue HMGB1 protein levels clearly decreased in an ad-miR141−dependent manner (Fig. 2C). Increasing the amount of injected pYr-adv-mmu-miR141 from 1×10^{10} PFU to 1.5×10^{10} PFU per mouse did not further decrease the pancreatic HMGB1 protein level. To evaluate the temporal pattern of HMGB1 expression after the hydrodynamics-based pYr-adv-mmu-miR141 delivery, samples were collected at various time points after the injection of pYr-adv-mmu-miR141 at 1×10^{10} PFU per mouse (Fig. 2D). The HMGB1 protein level in pancreatic tissue of mice with pYr-adv-mmu-miR141 treatment was at the lowest point 4 days after the injection, but increased a little at day 6 due to possible miRNA degradation. These results indicate that microRNA-141 is transfected in pancreatic tissues successfully and down-regulates the expression of HMGB1 after hydrodynamics-based pYr-adv-mmu-miRNA-141 delivery.

The model of acute pancreatitis is constructed successfully

As shown in Fig. 3, the pancreatic tissues were H&E stained and examined for fibrosis, parenchymal edema, inflammatory cell infiltration, acinar necrosis, and vacuolization, and were analyzed in 20 randomly selected fields (5 mice per group). As shown in Table 1, compared to Normal saline control mice, injection of L-arginine increased the overall average tissue injury score, indicating that acute pancreatitis is constructed successfully via intraperitoneal injections of L-arginine.

MicroRNA-141 protects against L-arginine-induced acute severe pancreatitis

As shown in Fig. 4, the pancreatic tissues were H&E stained and examined for fibrosis, parenchymal edema, inflammatory cell

Table 1
Histologic assessment of pancreatic tissue sections by quantification of the overall average tissue injury score.

Group	Fibrosis	Edema	Inflammation	Necrosis	Vacuoles	Average
NS	0 ± 0	0 ± 0	0 ± 0	0 ± 0	0 ± 0	0 ± 0
L-arginine	0 ± 0	0.47 ± 0.10	0.28 ± 0.05	0.30 ± 0.10	0.75 ± 0.15	0.36 ± 0.09*

Quantitation of the overall average tissue injury score, $p^* < 0.05$ vs NS group.

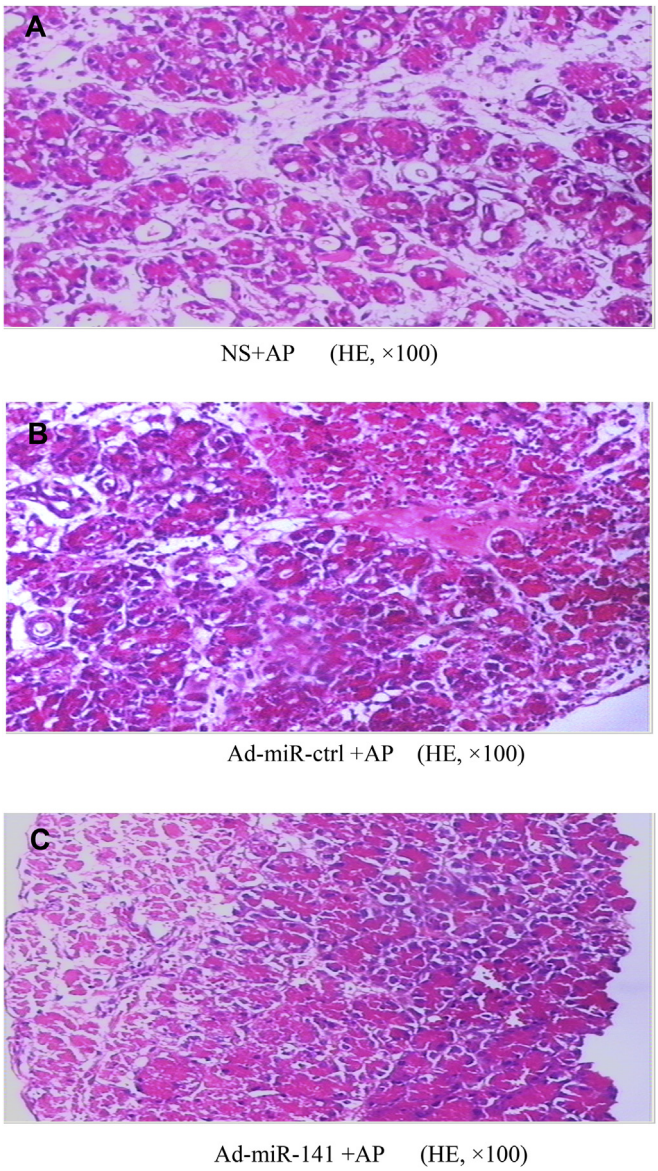

Fig. 4. Histologic assessment of acute pancreatitis tissues in response to L-arginine plus normal saline **(A)**, L-arginine plus Ad-miR-Ctrl **(B)** and L-arginine plus Ad-miR-141**(C)**, stained with H&E. Note the large areas of vacuoles within the acute pancreatitis tissue. Original magnification: 100×.

infiltration, acinar necrosis, and vacuolization, and were analyzed in 20 randomly selected fields (5 mice per group). The area of vacuoles within the acute pancreatitis tissue became smaller by using Ad-miR-141 treatment plus L-arginine, compared with L-arginine plus normal saline group. As shown in Table 2, Ad-miR-141 decreased the overall average tissue injury score in L-arginine-treated group compared to L-arginine plus normal saline group, indicating that the tissue injury using Ad-miR-141 treatment is much less than normal saline treatment.

Effects of miR-141 on regulation of autophagy in vivo

To further investigate the effects of miR-141 on regulation of autophagy in vivo, pancreatic tissues were treated for electron microscopy to assess the autophagosomal and autolysosomal formation (Fig. 5A-B). Compared with L-arginine plus normal saline group, autophagosomes and autolysosomes were evidently reduced in Ad-miR-141 treatment plus L-arginine group. Meanwhile, Ad-miR-141 decreased the expression of autophagy marker protein LC3-II in pancreatic tissues of mice in the L-arginine group compared to L-arginine plus normal saline group (Fig. 5C). Furthermore, the p62, which is degraded by autolysosomal, was relative up-regulated in the L-arginine plus Ad-miR-141 group compared to the L-arginine plus normal saline group (Fig. 5D). The Lamp-2, regulating the fusion of autophagosome with lysosome, had no significant differences between the L-arginine plus Ad-miR-141 and L-arginine plus normal saline (Fig. 5E). Taken together, autophagy is impaired in the L-arginine plus Ad-miR-141 group. Due to no difference of Lamp-2 protein, we may conclude that Ad-miR-141 inhibit the formation of autophagosome.

miR-141 may regulate autophagy through HMGB1/Beclin-1 pathway

Several evidences prove that cytosolic HMGB1 is a novel Beclin-1-binding protein that dissociates its inhibitory partner Beclin-2 to induce autophagy [19]. To verify the effects caused by Ad-miR-141 treatment, we detected the miR-141, HMGB1 mRNA, and Beclin-1 mRNA in pancreatic tissue by qRT-PCR (Fig. 6A). Compared with L-arginine plus normal saline group, the expression of miR-141 was increased sharply in L-arginine plus Ad-miR-141 group. Meanwhile, the HMGB1 mRNA and Beclin-1 mRNA in pancreatic tissue were obviously down-regulated in L-arginine plus Ad-miR-141 group. In addition, the protein of HMGB1 and Beclin-1 were determined by Western blot analysis (Fig. 6B). Compared with L-arginine plus normal saline group, the protein of HMGB1 and Beclin-1 level were significantly decreased in L-arginine plus Ad-miR-141 group. These results indicate that miR-141 may regulate autophagy through HMGB1/Beclin-1 pathway.

Of note, to evaluate potential drug toxicity on mice during the treatment, no pathological changes in heart, liver, spleen, lungs, or kidneys of treated mice were detected by microscopic examination.

Discussion

Autophagy is a catabolic process involving the degradation of a cell's own components, such as waste or excess proteins and organelles through the lysosomal machinery [20]. It is controlled by a large number of regulators, signalers and miRNAs [21–24]. In this study, it is shown that miR141 inhibits HMGB1 expression through a miR141-binding site within the 3′ UTR of HMGB1 mRNA, leading to translational repression of HMGB1 in mouse hepal-6 cell.

Table 2
Histologic assessment of pancreatic tissue sections by quantification of the overall average tissue injury score.

Group	Fibrosis	Edema	Inflammation	Necrosis	Vacuoles	Average
NS + AP	0 ± 0	0.50 ± 0.10	0.25 ± 0.05	0.35 ± 0.07	0.75 ± 0.14	0.37 ± 0.07
Ad-miR-ctrl + AP	0 ± 0	0.50 ± 0.18	0.30 ± 0.15	0.30 ± 0.05	0.70 ± 0.12	0.36 ± 0.10
Ad-miR-141 + AP	0 ± 0	0.10 ± 0.05	0.10 ± 0.02	0.10 ± 0.03	0.30 ± 0.05	0.12 ± 0.03*

Quantitation of the overall average tissue injury score, AP, acute pancreatitis. $P^* < 0.05$ vs L-arginine plus normal saline group.

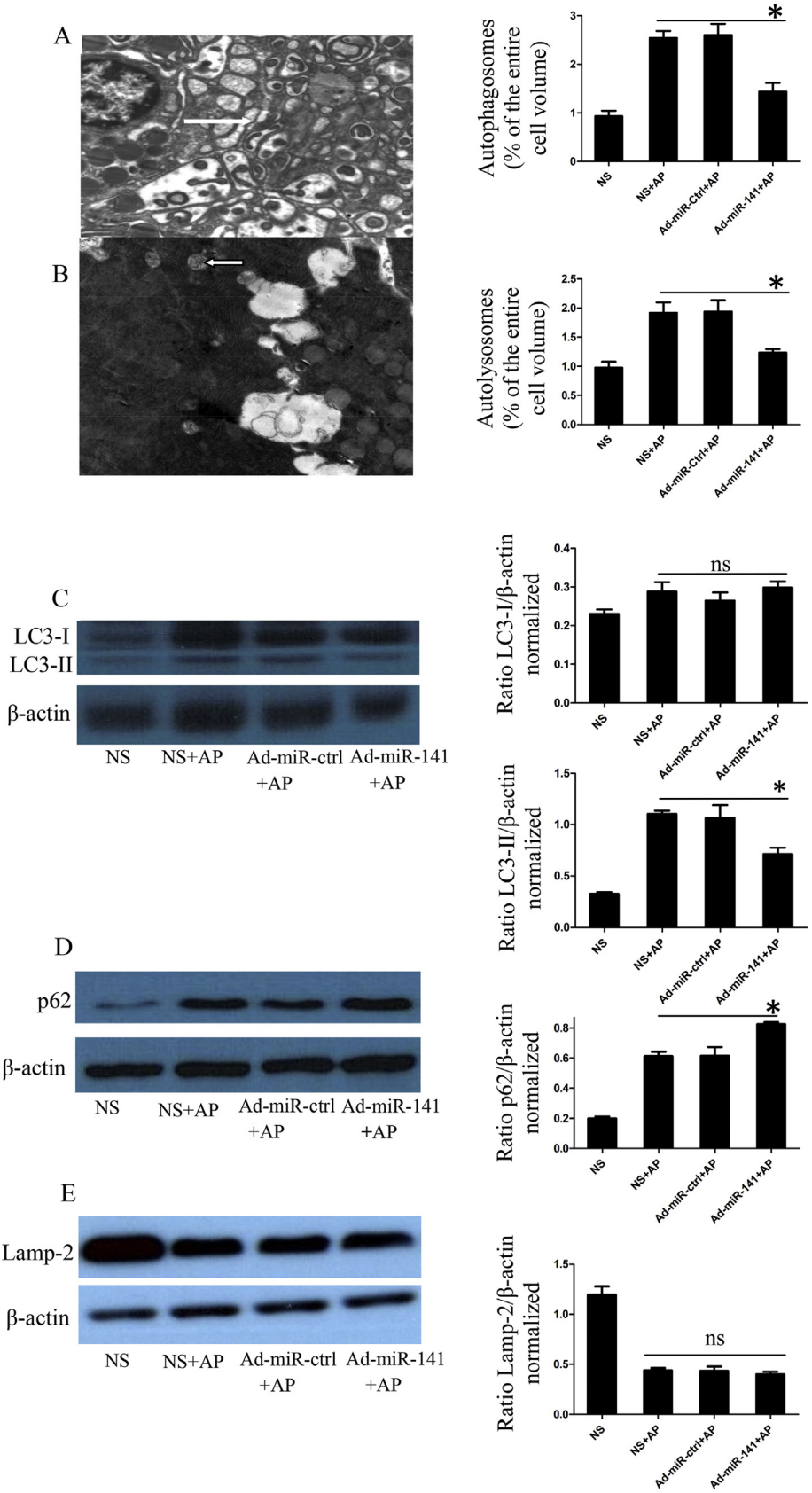

Fig. 5. The effects of miR-141 on regulation of autophagy. **(A)** Representative EM image of pancreatic acinar cells. The white arrow indicates a typical autophagosome containing mitochondria and other intracellular components. Scale bar: 2 μm. **(B)** Representative EM image of pancreatic acinar cells. The white arrow indicates a typical autolysosome containing digested mitochondria and other intracellular components. Scale bar: 2 μm. Quantitation of autophagosomes and autolysosome determined as percentage of the entire acinar cell volume, plotted as mean ± SD of 4 cells per group. $^{*}P < 0.05$ vs L-arginine plus normal saline. **(C)** Protein expression of LC3-II was determined by western blot analysis ($n = 5$; $P < 0.05$ versus L-arginine plus normal saline). **(D)** Protein expression of p62 was determined by western blot analysis ($n = 5$; $P < 0.05$ versus L-arginine plus normal saline). (**E**) Protein expression of Lamp-2 was determined by western blot analysis ($n = 5$; $P < 0.05$ versus L-arginine plus normal saline).

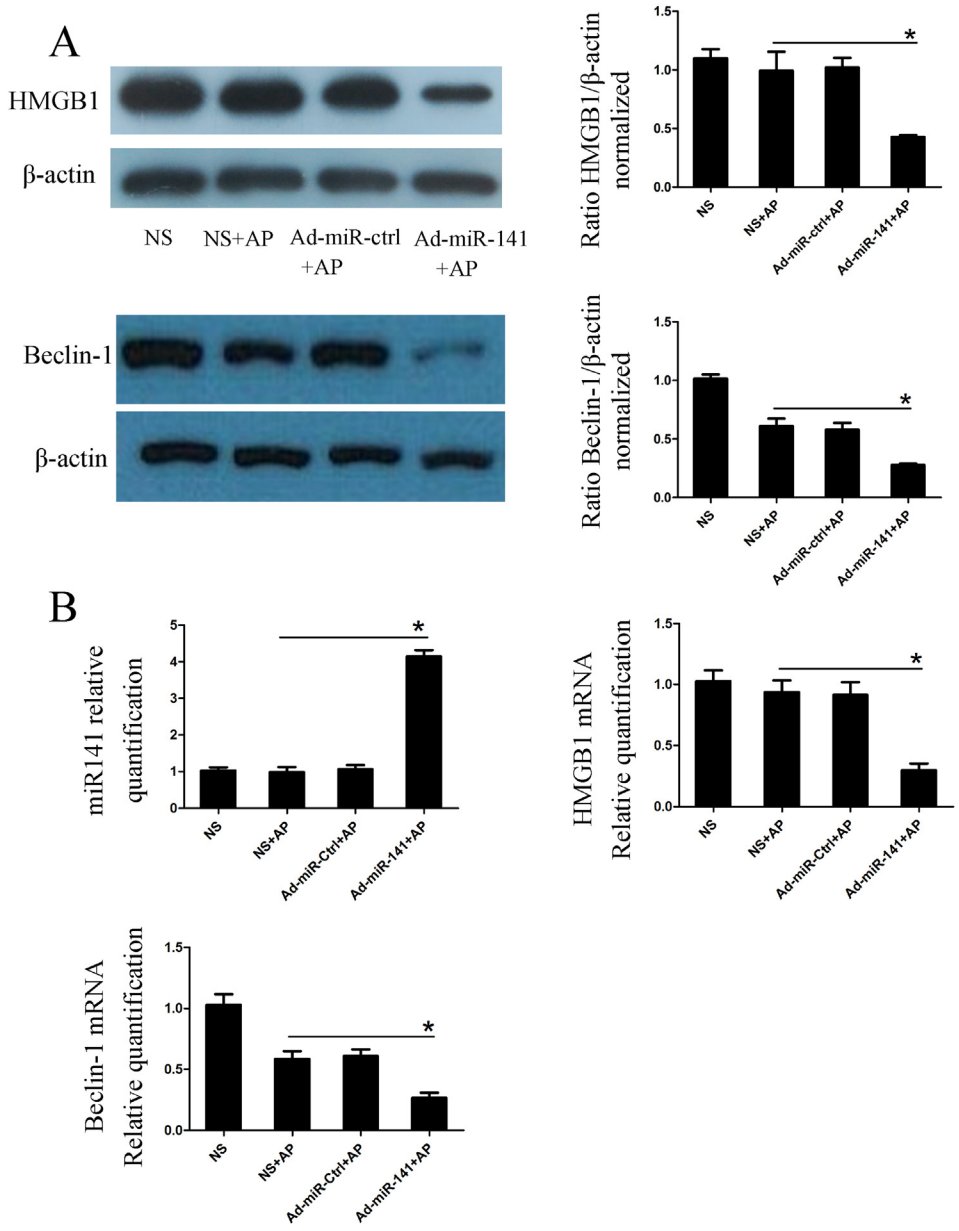

Fig. 6. The expression of HMGB1 and Beclin-1 level were down-regulated after miR-141 administration. **(A)** Expressions of HMGB1 and Beclin-1 were evidently decreased in pancreatic tissue treated with Ad-miR-141 in L-arginine group analyzing by Western blotting ($n = 5$; $P < 0.05$ vs. L-arginine plus normal saline group). **(B)** The miR-141, HMGB1 and Beclin-1 relative quantification of each group in pancreatic tissues were detected by qRT-PCR in vivo. Ad-miR-141 decreased sharply the expression of HMGB1 and Beclin-1 in L-arginine group (n = 5; $P < 0.05$ vs. L-arginine plus normal saline group).

The present study demonstrates that the hydrodynamics-based gene delivery by intravenous administration of microRNA can provide an efficient and useful approach for expressing gene in vivo. Obviously, an efficient method for gene delivery in pancreatic acinar cells would be a useful tool for genetic lineage tracing, overexpression and knock-down studies and for gene therapy. Several viral vectors such as adenoviral vectors [25–27], lentiviral vectors [28–30] and adeno-associated viral vectors (AAV) [31–33] have been used for gene delivery in pancreas. The present data proves that transfection of pancreatic exocrine cells requires lentiviral vectors in vitro but adenoviral vectors in vivo [34]. Because the purpose of our study is to knock-down HMGB1 by systemic administration of microRNA-141 in vivo, we choose the adenoviral vectors for gene therapy by intravenous administration of microRNA-141. Our results indicate that high levels of pancreatic miR141 could be obtained after the delivery of pYr-adv-mmu-miR141 using a hydrodynamics-based approach and that the high levels could be sustained for a long period (at least 6 days) following a single injection. It means that pYr-adv-mmu-miR-141 is transfected in vivo successfully. In addition, HMGB1 protein expression was knocked down with the up-regulation of miR-141 after the delivery of pYr-adv-mmu-miR-141.

Several evidences prove that the efficiency of autophagic flux depends primarily on the rates of the formation of autophagosome and the degradative activity of autolysosomes, the latter being controlled by the levels of Lamp-2. As we all know that the number of autophagosomes observed at any time reflects the balance between the rates of their generation and degradation during the subsequent stages of autophagy. P62 is localized at the autophagosome formation site [35] and directly interacts with LC3, an

autophagosome location protein [36–39]. In this context, p62 is incorporated into the autophagosome and then degraded through autophagy. Our results demonstrated that the autophagy marker LC3-II, an autophagosome location protein, was decreased in L-arginine plus Ad-miR-141 group compared to the L-arginine plus normal saline group, In addition, autophagosomal formation is decreased by electron microscopy. Taken together, Ad-miR-141 can block the process of autophagosomal formation. Furthermore, the autophagy marker p62 protein expression in pancreatic tissues was relatively increased in L-arginine plus Ad-miR-141 group indicating that the relative down-regulated expression of autolysosomes, which is corresponded with the result of electron microscopy. These finding suggest that autophagy is impaired in the L-arginine plus Ad-miR-141 group. Of note, the Lamp-2, regulating the fusion of lysosome with autophagosome, had no significant difference between the L-arginine plus Ad-miR-141 group and L-arginine plus normal saline group, we may conclude that Ad-miR-141 inhibits the formation of autophagosome.

HMGB1, a conserved nuclear protein that enhances transcription, was recently discovered to be a crucial regulator of autophagy that mediates the stress response [40]. Recent evidence has demonstrated that activating the HMGB1 expression induces autophagy, and loss of endogenous HMGB1 inhibits autophagy in several cell types. HMGB1 plays subcellular localization-dependent roles in the regulation of autophagy. Cytosolic HMGB1 is a novel Beclin-1-binding protein that dissociates its inhibitory partner Beclin-2 to induce autophagy [19]. Moreover, ULK1 and TP53 positively and negatively regulate the interaction between HMGB1 and Beclin-1 in cancer cells respectively [41]. Extracellular HMGB1 binds to AGER/RAGE (advanced glycosylation end product-specific receptor), but not TLR4, which inhibits mTOR and promotes the formation of Beclin-1-PIK3C3 core autophagic complexes in cancer cells. Our findings prove that miR-141 inhibits HMGB1 expression and reduces its protein levels, moreover, the level of Beclin-1 is also decreased with the down-regulation of HMGB1, suggesting that miR-141 may regulate autophagy through the HMGB1/Beclin-1 pathway.

Our results demonstrate that miR-141 inhibits HMGB1 expression through a miR141-binding site within the 3′UTR of HMGB1 mRNA. Inhibition of HMGB1 by miR-141 may block the process of autophagosome formation through the HMGB1/Beclin-1 pathway. For the first time miR-141 was applied in acute pancreatitis treatment in vivo. Since intrinsic miRNA may be better in acting on genes with similar functions, the plasmid-mediated miR-141 appears to be a promising candidate for the gene therapy of acute pancreatitis.

Disclosure statement

None.

Acknowledgment

The project was supported by the National Natural Science Foundation of China (Grant No. 81570585, 81270545), the Science and Technology Department of Hunan Province Foundation of China (Grant No. 2013FJ6021), and the Hunan Provincial Natural Science Foundation of China (Grant No. 12JJ5052).

References

[1] Bartel DP. MicroRNAs: genomics, biogenesis, mechanism,and function. Cell 2004;116(2):281–97.
[2] Narry Kim V, Nam Jin-Wu. Genomics of microRNA. Trends Genet 2006;22(13):165–73.
[3] Carrington JC, Ambros V. Role of microRNAs in plant and animal development. Science 2003;301(5631):336–8.
[4] Ambros V. The functions of animal microRNAs. Nature 2004;431(7006):350–5.
[5] Chen JF, Mandel EM, Thomson JM, Wu Q, Callis TE, Hammond SM, et al. The role of microRNA-1 and microRNA-133 in skeletal muscle proliferation and differentiation. Nat Genet 2006;38(2):228–33.
[6] Cheng AM, Byrom MW, Shelton J, Ford LP. Antisense inhibition of human miRNAs and indications for an involvement of miRNA in cell growth and apoptosis. Nucleic Acids Res 2005;33(4):1290–7.
[7] Kloosterman WP, Plasterk RH. The diverse functions of microRNAs in animal development and disease. Dev Cell 2006;11(4):441–50.
[8] Jiang J, Yamato E, Miyazaki J. Intravenous delivery of naked plasmid DNA for in vivo cytokine expression. Biochem Biophys Res Commun 2001;289(5):1088–92.
[9] Wang W, Dai LX, Zhang S, Yang Y, Yan N, Fan P, et al. Regulation of epidermal growth factor receptor signaling by plasmid-based MicroRNA-7 inhibits human malignant gliomas growth and metastasis invivo. Neoplasma 2013;60(3):274–83.
[10] Pandol SJ, Saluja AK, Imrie CW, Banks PA. Acute pancreatitis: bench to the bedside. Gastroenterology 2007;132(3):1127–51.
[11] Lotze MT, Tracey KJ. High-mobility group box 1 protein (HMGB1): nuclear weapon in the immune arsenal. Nat Rev Immunol 2005;5(4):331–42.
[12] Harris HE, Andersson U, Pisetsky DS. HMGB1: a multifunctional alarm in driving autoimmune and inflammatory disease. Nat Rev Rheumatol 2012;8(4):195–202.
[13] Yasuda T, Ueda T, Takeyama Y, Shinzeki M, Sawa H, Nakajima T, et al. Significant increase of serum high-mobility group box chromosomal protein 1 levels in patients with severe acute pancreatitis. Pancreas 2006;33(4):359–63.
[14] Kocsis AK, Szabolcs A, Hofner P, Takacs T, Farkas G, Boda K, et al. Plasma concentrations of high-mobility group box protein 1, soluble receptor for advanced glycation end-products and circulating DNA in patients with acute pancreatitis. Pancreatology 2009;9(4):383–91.
[15] Yasuda T, Ueda T, Shinzeki M, Sawa H, Nakajima T, Takeyama Y, et al. Increase of high-mobility group box chromosomal protein 1 in blood and injured organs in experimental severe acute pancreatitis. Pancreas 2007;34(4):487–8.
[16] Cheng BQ, Liu CT, Li WJ, Fan W, Zhong N, Zhang Y, et al. Ethyl pyruvate improves survival and ameliorates distant organ injury in rats with severe acute pancreatitis. Pancreas 2007;35(3):256–61.
[17] Sawa H, Ueda T, Takeyama Y, Yasuda T, Shinzeke M, Nakajima T, et al. Blockade of high mobility group box-1 protein attenuates experimental severe acute pancreatitis. World J Gastroenterol 2006;12(47):7666–70.
[18] Yuan H, Jin X, Sun J, Li F, Feng Q, Zhang C, et al. Protective effect of HMGB1 a box on organ injury of acute pancreatitis in mice. Pancreas 2009;38(2):143–8.
[19] Tang D, Kang R, Livesey KM, Cheh CW, Farkas A, Loughran P, et al. Endogenous HMGB1 regulates autophagy. J Cell Biol 2010;190(5):881–92.
[20] Mizushima N, Levine B, Cuervo AM, Klionsky DJ. Autophagy fights disease through cellular self-digestion. Nature 2008;451(7182):1069–75.
[21] He C, Klionsky DJ. Regulation mechanisms and signaling pathways of autophagy. Annu Rev Genet 2009;43:67–93.
[22] Kroemer G, Mari G, Levine B. Autophagy and the integrated stress response. Mol Cell 2010;40(2):280–93.
[23] Frankel LB, Lund AH. MicroRNA regulation of autophagy. Carcinogenesis 2012;33(11):2018–25.
[24] Xu J, Wang Y, Tan X, Jing H. MicroRNAs in autophagy and their emerging roles in crosstalk with apoptosis. Autophagy 2012;8:873–82.
[25] Wang AY, Ehrhardt A, Xu H, Kay MA. Adenovirus transduction is required for the correction of diabetes using Pdx-1 or Neurogenin-3 in the liver. Mol Ther 2007;15(2):255–63.
[26] Wang AY, Peng PD, Ehrhardt A, Storm TA, Kay MA. Comparison of adenoviral and adeno-associated viral vectors for pancreatic gene delivery in vivo. Hum Gene Ther 2004;15(4):405–13.
[27] Zhang L, Graziano K, Pham T, Logsdon CD, Simeone DM. Adenovirus mediated gene transfer of dominant-negative Smad4 blocks TGF-beta signaling in pancreatic acinar cells. Am J Physiol Gastrointest Liver Physiol 2001;280(6):G1247–53.
[28] Chou FC, Sytwu HK. Overexpression of thioredoxin in islets transduced by a lentiviral vector prolongs graft survival in autoimmune diabetic NOD mice. J Biomed Sci 2009;16:71.
[29] He Z, Wang F, Kumagai-Braesch M, Permert J, Holgersson J. Long-term gene expression and metabolic control exerted by lentivirus-transduced pancreatic islets. Xenotransplantation 2006;13(3):195–203.
[30] Kobinger GP, Deng S, Louboutin JP, Vatamaniuk M, Matschinsky F, Markmann JF, et al. Transduction of human islets with pseudotypedlentiviral vectors. Hum Gene Ther 2004;15(2):211–9.
[31] Cheng H, Wolfe SH, Valencia V, Qian K, Shen L, Phillips MI, et al. Efficient and persistent transduction of exocrine and endocrine pancreas by adeno-associated virus type 8. J Biomed Sci 2007;14(5):585–94.
[32] Jimenez V, Ayuso E, Mallol C, Agudo J, Casellas A, Obach M, et al. In vivo genetic engineering of murine pancreatic beta cells mediated by single-stranded adeno-associated viral vectors of serotypes 6, 8 and 9. Diabetologia 2011;54(5):1075–86.
[33] Wang Z, Zhu T, Rehman KK, Bertera S, Zhang J, Chen C, et al. Widespread and stable pancreatic gene transfer by adeno-associated virus vectors via different routes. Diabetes 2006;55(4):875–84.

[34] Houbracken I, Baevens L, Ravassard P, Heimberg H, Bouwens L. Gene delivery to pancreatic exocrine cells in vivo and in vitro. BMC Biotechnol 2012;12:74.
[35] Itakura E, Mizushima N. SQSTM1 targeting to the autophagosome formation site requires self-oligomerization but not LC3 binding. J Cell Biol 2011;192(1):17–27.
[36] Ichimura Y, Kumanomidou T, Sou YS, Mizushima T, Ezaki J, Ueno T, et al. Structural basis for sorting mechanism of SQSTM1 in selective autophagy. J Biol Chem 2008;283:22847–57.
[37] Noda NN, Kumeta H, Nakatogawa H, Satoo K, Adachi W, Ishii J, et al. Structural basis of target recognition by Atg8/LC3 during selective autophagy. Genes Cells 2008;13(12):1211–8.
[38] Pankiv S, Clausen TH, Lamark T, Brech A, Outzen H, Overvatn A, et al. SQSTM1/SQSTM1 binds directly to Atg8/LC3 to facilitate degradation of ubiquitinated protein aggregates by autophagy. J Biol Chem 2010;282(33):24131–45.
[39] ShvetsE FassE, Scherz-Shouval R, Elazar Z. The N-terminus and Phe52 residue of LC3 recruit SQSTM1/SQSTM1 into autophagosomes. J Cell Sci 2008;121(Pt16):2685–95.
[40] Tang D, Kang R, Coyne CB, Zeh HJ, Lotze MT. PAMPs and DAMPs: signal 0s that spur autophagy and immunity. Immunol Rev 2012;249(1):158–75.
[41] Huang J, Ni J, Liu K, Yu Y, Xie M, Kang R, et al. HMGB1 promotes drug resistance in osteosarcoma. Cancer Res 2012;72(1):230–8.